Struct Multidisc Optim (2013) 48:627–636
DOI 10.1007/s00158-013-0907-8

INDUSTRIAL APPLICATION

Topology optimization for a frequency response and its application to a violin bridge

Yonggyun Yu · In Gwun Jang · Byung Man Kwak

Received: 31 May 2012 / Revised: 16 December 2012 / Accepted: 6 February 2013 / Published online: 9 March 2013

Abstract The main role of a violin bridge is to hold the strings and to transmit the vibration of the strings to the violin body. Violin makers have been empirically aware of the fact that a bridge is an important element which influences violin timbre. Thus, a bridge can be regarded as a mechanical filter in the transmission and be used to compensate weak or too strong areas in the resonance of the violin body. The filtering characteristics of a bridge depend on the geometry and material distribution of the bridge. In this paper, the sensitivity of band-averaged frequency response with respect to geometric design variables is derived. Then, topology optimization is applied to obtain optimal violin bridges for desired filtering characteristics. Numerical results show that the proposed optimization process can be a viable tool to design a bridge according to prescribed characteristics for musical performance.

Keywords Violin bridge · Topology optimization · Frequency response · Musical instruments

1 Introduction

A violin bridge, a small wooden structure placed on the top plate of a violin (Fig. 1), has been considered an important part of a violin for centuries. At the first glance, the shape of a bridge with its holes looks very decorative and aesthetic, but is actually critical to the function of a bridge: tuning the quality of violin sounds. Acting as a mechanical filter for the various wavelengths of sound, a bridge transforms the transverse force from the vibrating string into normal forces applied to a violin body through the bridge feet resting at the position near the notches of the f-holes. Recent studies (Hutchins and Benade 1997; Jansson and Niewczyk 1999; Woodhouse 2005) reveal that violin bridges adjust the impedance characteristics for loudness and tonal color. Especially, Cremer showed that a violin bridge has internal resonances within the frequency range of interest for the sound of the instrument, so that the filtering effect of the bridge has significant variation with frequency (1983).

Many researchers also have tried to find out the relationship between the frequency response (sound spectrum) and quality of violin sound (timbre or tonal color) (Gabrielson and Jansson 1977; Moral and Jansson 1978; Dunnwald 1991; Hutchins and Benade 1997; Buen 2003, 2007; Geissler et al. 2003; Scheleske 2010; Stepanek and Otcenasek 1999, 2001, 2004, 2005). It has been reported that many excellent violins show a broad peak of response in the neighborhood of 3.0 kHz, which is called the "bridge hill" for the reason that the lowest bridge resonance is also found in the range of 3.0 kHz when the bridge feet are fixed (Jansson and Niewczyk 1999; Woodhouse 2005). As one of the most frequently cited research, Dunnwald suggested the important frequency ranges for the judgment of the sound quality by comparing frequency responses of various violins from factory violins to old Italian violins (1991). According to Dunnwald, the first range (190–650 Hz) is responsible for the content of lower overtones. If the second range (650–1300 Hz) is too strong, the instrument will sound boxy and

Y. Yu (✉)
Korea Atomic Energy Research Institute,
Daejeon 305-353, Republic of Korea
e-mail: YonggyunYu@kaist.ac.kr

I. G. Jang · B. M. Kwak
Korea Advanced Institute of Science and Technology,
Daejeon 305-701, Republic of Korea

I. G. Jang
e-mail: jangin0407@kaist.ac.kr

B. M. Kwak
e-mail: bmkwak@kaist.ac.kr

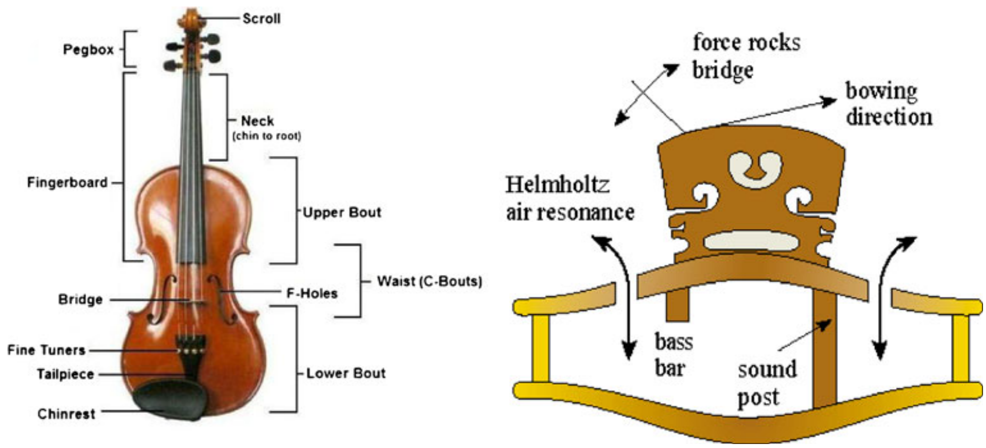

Fig. 1 Structure of violin body and violin bridge (Gough 2000)

nasal. The third range (1300–4200 Hz) gives the instrument brilliance and good radiation. The upper range (4200–6400 Hz) should be relatively low to clear sound. He defined the sound parameters such as loudness, clarity, and nasality by combining the averaged strengths within six frequency ranges as shown in Fig. 2 and Table 1.

The layout (or material distribution) of a bridge is important since an increase in thickness enhances its stability but requires more vibration energy of strings for transmitting. It also affects the resonance of a bridge, which boosts the intensity of any partials (a combination of many simple periodic waves, each with its own frequency of vibration, amplitude and phase) in this frequency range and therefore changes sound quality. As Müller stated that there is no ideal bridge but there is ideally suitable bridge for given instruments and the taste of players, a bridge can be individually tailored to the taste of instrument's owner by changing its geometric shape (1979). The tuning of a violin bridge to date, however, has been fully based on violin maker's experiences and intuition instead of scientific bases. To the authors' knowledge, little literature has been published about systematically designing the optimal layout of a bridge (e.g., size, shape, and location of holes) for its musical performance.

Question on the "optimal" layout of a bridge could be answered by applying design optimization, especially topology optimization. Unlike size and shape optimization, topology optimization is available in determining the optimal layout (or topology) of a given structure by creating or deleting holes while improving the given objective function during the process. In the so-called density-based topology optimization (Bendsoe 1989; Yang and Chuang 1994; Borvall and Petersson 2001; Jang and Kwak 2006, 2008), the design domain is discretized by finite elements, and the density of each element is used as a design variable. Young's Modulus of each element can be formulated with several different interpolation models in terms of element density (Bendsoe and Sigmund 2003; Stolpe and Svanberg 2001; Pedersen 2000).

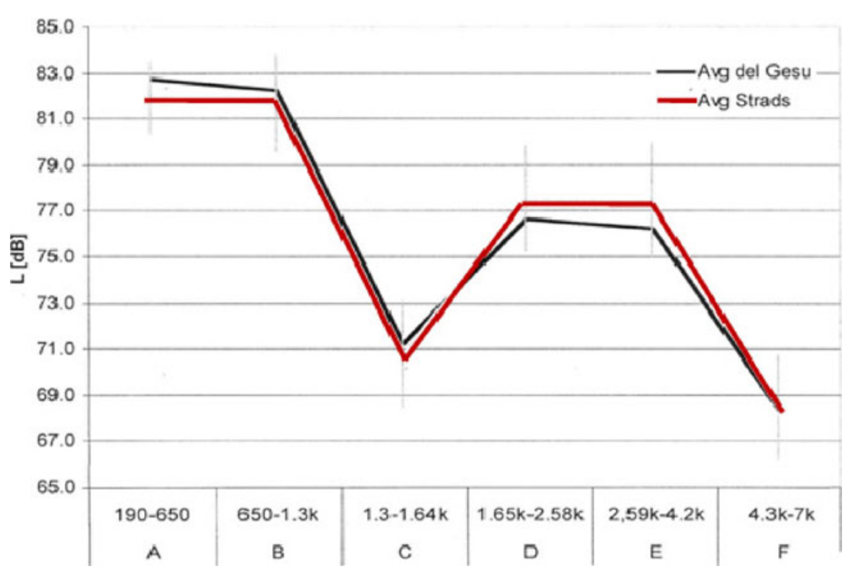

Fig. 2 Levels of each Dunnwald frequency band for the average long-time-average spectra (Buen 2007)

Table 1 Dunnwald parameters for violin timbre (Buen 2007)

Timbre parameter	Definition	Comment
Bass	ave(A) – ave(B)	High values for good and bass-rich violins
Nasality	ave(A, C, D)[a] – ave(B)	High value for 'non nasal' violins Low values for 'nasal' violin
Clarity	ave(D, E) – ave(F)	High values for 'clear' violins Low values for 'harsh' sound

[a]ave(A, C, D) denotes the averaged response in the ranges of A, C, and D

Since the 1990's, topology optimization has been applied successfully to various mechanical problems including mechanical filters and resonators (Ma et al. 1993, 1995a, b; Silva et al. 2000; Yoo and Kikuchi 2002). From the engineering viewpoint, the design of a violin bridge is conceptually similar to that of mechanical filters or resonator because resonant properties and filtering characteristics are critical in their design. However, the design of a violin bridge is more complicated as follows:

- Concurrent designs: For meaningful design of a violin bridge, many aspects should be considered concurrently: rigidity (i.e. compliances with various loading conditions), dynamic properties (eigenfrequencies and eigenmodes), mass, and frequency response.
- Frequency domain response for sound quality: The bridge design is necessary to consider the frequency response in the range of audible frequency, not for any single frequency. The shape of frequency response curve (also known as spectral envelope) has close relationship with sound quality. Thus, sound quality should be quantified, and other filtering characteristics desired should be determined prior to optimization.

While topology optimization for static response or single eigenfrequency is relatively easy to perform, it is still challenging to apply topology optimization to problems concerning frequency response in the specified range. In traditional density based approaches (Bendsoe 1989; Yang and Chuang 1994; Borvall and Petersson 2001), the system matrix should be updated for each frequency, and thus it causes high computational cost. The modal approaches (Ma et al. 1993, 1995a, b) typically lead to non-smooth optimization problem that might pose difficulties in convergence for optimization algorithm. In order to overcome the difficulties of modal approaches, Jensen proposed the method which uses a Pade function to approximate a frequency response function (2007). Recently, Yoon proposed a new modal method based on Ritz vectors, and compared it with conventional modal approaches (2010).

In this paper, we proposed, for the first time to our knowledge, the systematic design framework for a violin bridge. We first set the quantitative measures to define the sound quality, and proposed an efficient spline-based method to obtain the frequency response with the aid of approximated stiffness and mass matrices. After deriving sensitivities of the measures selected in the paper, we applied them to topology optimization to obtain an optimized violin bridge in terms of sound quality. Numerical results showed the possibility of tailoring a violin bridge to one's own taste by virtue of optimization, not violin maker's experiences and intuition. More accurate FE analysis and experiments with psychoacoustic test would be followed in further work.

2 Theoretical derivation

2.1 Basic finite element analysis

The equation for the structural response of a given system may be expressed in the following form:

$$\mathbf{M}\ddot{\mathbf{u}} + \mathbf{C}\dot{\mathbf{u}} + \mathbf{K}\mathbf{u} = \mathbf{f} \tag{1}$$

where $\mathbf{u}$, $\mathbf{M}$, $\mathbf{C}$, $\mathbf{K}$, and $\mathbf{f}$ are the generalized displacement vector, mass matrix, damping matrix, stiffness matrix, and force vector, respectively. For a frequency response problem, assuming $\mathbf{f} = \mathbf{f}_0 e^{j\omega t}$ and $\mathbf{u} = \mathbf{u}_0 e^{j\omega t}$, we have

$$\left(-\omega^2\mathbf{M} + j\omega\mathbf{C} + \mathbf{K}\right)\mathbf{u}_0 = \mathbf{f}_0 \tag{2}$$

$$\mathbf{S} = -\omega^2\mathbf{M} + j\omega\mathbf{C} + \mathbf{K} \tag{3}$$

where $\mathbf{S}$ is called as a dynamic stiffness matrix. To solve a topology optimization problem, sensitivities of the objective and constraint functions with respect to design variable, ρ_e, are required. Candidates for objective and constraint functions in this paper are static and harmonic responses. Then, the functions can be described in the simple form as

$$\psi = \boldsymbol{\alpha}^T\mathbf{u}_0 \tag{4}$$

where $\boldsymbol{\alpha}$ is a design independent vector and $\mathbf{u_0}$ is static or harmonic response. In the case of static analysis, the sensitivities of static response, $\boldsymbol{\alpha}^T\mathbf{u}_0$, is computed as (Choi and Kim 2005)

$$\frac{d\psi}{db} = \bar{\boldsymbol{\lambda}}^T\left(\frac{\partial \mathbf{f}_0}{\partial b} - \frac{\partial \mathbf{K}}{\partial b}\mathbf{u}\right) \tag{5}$$

where $\boldsymbol{\lambda}$ is an adjoint variable which can be calculated from the adjoint equation, $\mathbf{K}\boldsymbol{\lambda} = \boldsymbol{\alpha}$. The sensitivity for a harmonic analysis problem is obtained similarly to that of static analysis as follows:

$$\frac{d\psi}{db} = \overline{\boldsymbol{\lambda}}^T \frac{\partial \mathbf{f}_0}{\partial b} - \overline{\boldsymbol{\lambda}}^T \left(\frac{\partial \mathbf{S}}{\partial b}\right)\mathbf{u}_0$$

$$= \overline{\boldsymbol{\lambda}}^T \frac{\partial \mathbf{f}_0}{\partial b} - \overline{\boldsymbol{\lambda}}^T \left(\frac{\partial \mathbf{K}}{\partial b} + i\omega\frac{\partial \mathbf{C}}{\partial b} - \omega^2\frac{\partial \mathbf{M}}{\partial b}\right)\mathbf{u}_0 \tag{6}$$

where $\overline{\boldsymbol{\lambda}}$ is a complex conjugate of $\boldsymbol{\lambda}$ calculated from $\mathbf{S}\boldsymbol{\lambda} = \boldsymbol{\alpha}$. When the energy dissipation is characterized by the Rayleigh damping, damping matrix $\mathbf{C}$ in (6) can be expressed as

$$\mathbf{C} = \alpha\mathbf{M} + \beta\mathbf{K} \tag{7}$$

2.2 Band averaged frequency response

As explained in Section 1, sound quality can be quantified by combining the averaged frequency responses of some important frequency ranges. In order to calculate the average strength in the given frequency ranges, we consider the integrals of the harmonic response within a certain frequency domain as follows:

$$R = \int_{\omega 1}^{\omega 2} \left|\boldsymbol{\alpha}^T \mathbf{u}\right| d\omega = \int_{\omega 1}^{\omega 2} \sqrt{\left(\boldsymbol{\alpha}^T \mathbf{u}_{\mathrm{real}}\right)^2 + \left(\boldsymbol{\alpha}^T \mathbf{u}_{\mathrm{img}}\right)^2} d\omega \tag{8}$$

For numerical integration, a frequency response curve is approximated by a cubic spline curve in this paper (Fig. 3). In order to represent the peaks of the response curve more accurately, eigenfrequencies placed within the given ranges are inserted as additional control points. Given n frequencies, ω_i ($\omega_1 < \omega_2 < \ldots < \omega_{n-1} < \omega_n$), a cubic spline function, $\xi(\omega)$, is defined as follows:

$$\xi(\omega) = \begin{cases} \xi_1(\omega) & \textit{when } \omega \in [\omega_1, \omega_2] \\ \xi_2(\omega) & \textit{when } \omega \in [\omega_2, \omega_3] \\ \vdots & \\ \xi_{n-1}(\omega) & \textit{when } \omega \in \left[\omega_{n-1}, \omega_n\right] \end{cases} \tag{9}$$

In (9), the piecewise spline curve, $\xi_i(\omega)$, is defined as

$$\xi_i(\omega) = \frac{\zeta_{i+1}(\omega-\omega_i)^3 + \zeta_1(\omega_{i+1}-\omega)^3}{6h_i} + \left(\frac{f(\omega_{i+1})}{h_i} - \frac{h_i}{6}\zeta_{i+1}\right)(\omega-\omega_i) + \left(\frac{f(\omega_i)}{h_i} - \frac{h_i}{6}\zeta_i\right)(\omega_{i+1}-\omega) \tag{10}$$

where $f(\omega_i) = |\boldsymbol{\alpha}^T \mathbf{u}(\omega_i)|$, $h_i = \omega_{i+1} - \omega_i$, and ζ_i is the second order derivatives of spline curves with respect to the frequency of a control point, ω_i. In (10), ζ_i can be calculated by solving the following matrix:

$$\mathbf{P}\zeta = \mathbf{q} \tag{11}$$

where

$$\mathbf{P} = \begin{bmatrix} 2(h_1+h_2) & h_2 & & & & \\ h_2 & 2(h_2+h_3) & h_3 & & & \\ & h_3 & 2(h_3+h_4) & h_4 & & \\ & & \ddots & \ddots & \ddots & \\ & & & h_{n-3} & 2(h_{n-3}+h_{n-2}) & h_{n-2} \\ & & & & h_{n-2} & 2(h_{n-2}+h_{n-1}) \end{bmatrix},$$

$$\zeta = \begin{bmatrix} \zeta_1 \\ \zeta_2 \\ \zeta_3 \\ \vdots \\ \zeta_{n-2} \\ \zeta_{n-1} \end{bmatrix},$$

$$\text{and } \mathbf{q} = \begin{bmatrix} 6(b_2-b_1) \\ 6(b_3-b_2) \\ 6(b_4-b_3) \\ \vdots \\ 6(b_{n-2}-b_{n-3}) \\ 6(b_{n-1}-b_{n-2}) \end{bmatrix} \tag{12}$$

where $b_i = \frac{f(\omega_{i+1})-f(\omega_i)}{h_i} - \frac{f(\omega_i)-f(\omega_{i-1})}{h_{i-1}}$.

From (8), the average frequency response within the frequency range $[\alpha, \beta]$ can be represented using the approximated spline curve as

$$R = \frac{1}{\beta} = \alpha \int_{\alpha}^{\beta} \zeta(\omega)\, d\omega = \frac{1}{\beta-\alpha}\sum_{i=1}^{n-1}\int_{x_i}^{x_{i+1}} \zeta_i(\omega) d\omega = \frac{1}{\beta-\alpha}\sum_{i=1}^{n-1}\left(\frac{(\zeta_{i+1}-\zeta_i)(\omega_{i+1}-\omega_i)^4}{24h_i} + \left(\frac{f(\omega_{i+1})-f(\omega_i)}{h_i} - \frac{h_i}{6}(\zeta_{i+1}-\zeta_i)\right) \times (\omega_{i+1}-\omega_i)^2\right) \tag{13}$$

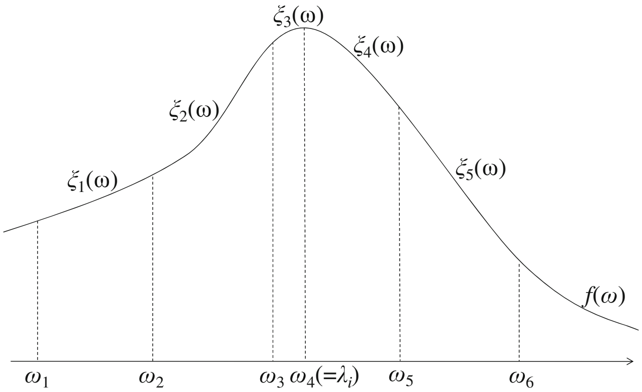

Fig. 3 Spline approximation of frequency response curve

Then, the sensitivity of the average response R is

$$\frac{\partial R}{\partial b} = \frac{1}{\beta-\alpha}\sum_{i=1}^{n-1}\left(\frac{\left(\frac{\partial}{\partial b}\zeta_{i+1}-\frac{\partial}{\partial b}\zeta_i\right)(\omega_{i+1}-\omega_i)^4}{24h_i} + \left(\frac{\frac{\partial}{\partial b}f(\omega_{i+1})-\frac{\partial}{\partial b}f(\omega_i)}{h_i} - \frac{h_i}{6}\left(\frac{\partial}{\partial b}\zeta_{i+1}-\frac{\partial}{\partial b}\zeta_i\right)\right) \times (\omega_{i+1}-\omega_i)^2\right) \tag{14}$$

where $\partial\zeta/\partial b$ and $\partial f(\omega_i)/\partial b$ are obtained by solving (15) and (16).

$$\mathbf{P}\frac{\partial \zeta}{\partial b} = \frac{\partial \mathbf{q}}{\partial b} \tag{15}$$

$$\begin{aligned}\frac{\partial f(\omega_i)}{\partial b} &= \frac{\mathrm{d}\left|\boldsymbol{\alpha}^T\mathbf{u}(\omega_i)\right|}{\mathrm{d}b}\\ &= \frac{\mathrm{d}}{\mathrm{d}b}\sqrt{\left(\boldsymbol{\alpha}^T\mathrm{Re}(\mathbf{u})\right)^2+(\boldsymbol{\alpha}^T\mathrm{Im}(\mathbf{u}))^2}\\ &= \frac{(\boldsymbol{\alpha}^T\mathrm{Re}(\mathbf{u}))\mathrm{Re}\left(\frac{\mathrm{d}(\boldsymbol{\alpha}^T\mathbf{u})}{\mathrm{d}b}\right)+(\boldsymbol{\alpha}^T\mathrm{Im}(\mathbf{u}))\mathrm{Im}\left(\frac{\mathrm{d}(\boldsymbol{\alpha}^T\mathbf{u})}{\mathrm{d}b}\right)}{|\boldsymbol{\alpha}^T\mathbf{u}|}\end{aligned} \tag{16}$$

Particularly, when the sampling frequency is an eigenfrequency, (17, 18) instead of (10) should be used to calculate the sensitivity of a dynamic stiffness matrix, $\mathbf{S}$, since an eigenfrequency varies with respect to design changes.

$$\mathbf{S}(\omega_p) = -\omega_p^2\mathbf{M} + j\omega_p\mathbf{C} + \mathbf{K} \tag{17}$$

$$\frac{\mathrm{d}\mathbf{S}(\omega_p)}{\mathrm{d}b} = \left(\frac{\partial \mathbf{K}(\omega_p)}{\partial b} + i\omega_p\frac{\partial \mathbf{C}(\omega_p)}{\partial b} - \omega_p^2\frac{\partial \mathbf{M}(\omega_p)}{\partial b}\right) + \frac{\mathrm{d}\omega_p}{\mathrm{d}b}\left(-2\omega_p\mathbf{M}(\omega_p)+j\mathbf{C}(\omega_p)\right) \tag{18}$$

where the sensitivity of ω_p is calculated by Choi and Kim (2005).

$$\frac{\partial \omega_p}{\partial b} = \frac{\partial \omega_p}{\partial \lambda_j}\frac{\partial \lambda_j}{\partial b} = \frac{1}{8\pi^2\omega_p}\left(\boldsymbol{\Phi}_j^T\frac{\partial \mathbf{K}}{\partial b}\boldsymbol{\Phi}_j - (2\pi\omega_p)^2\boldsymbol{\Phi}_j^T\frac{\partial \mathbf{M}}{\partial b}\boldsymbol{\Phi}_j\right) \tag{19}$$

If an objective or constraint function is defined based on a fixed modal order, the corresponding sensitivities may be discontinuous when mode switching happens, and an incorrect eigenmode may be optimized. In order to keep tracking the target modes, a mode assurance criterion (Kim and Kim 2000) is utilized in this paper. Also, for each element, the stiffness and mass matrices depend on only a small number of design variables that are associated with the given element (element density in this paper). Therefore, the derivative of a response function is simply calculated element-wise. The problem is, however, that the exact shape functions of the shell elements in commercial software are not open to the general public. This prohibits the development of any kind of analytic methods for obtaining sensitivity values. In our previous works (Yu et al. 2010; Yu and Kwak 2011), we proposed a regression model of stiffness and mass matrices of each element for deriving sensitivities. Same regression model for **M**, **C**, and **K** in (18) is also used in this paper. Check the detailed procedure in the reference.

3 Topology optimization of a violin bridge

3.1 Design domain and boundary condition

Figure 2 shows the design domain and boudnary condition for a violin bridge. The shape of upper and lower edges (lines 2–3 and lines 0–1 in Fig. 4, respectively) of a bridge are obtained from the conventional bridges. Design domain is represented as white in Fig. 4. The interaction between a bridge and a body is simply modeled using linear spring elements in this study. Generally, the stiffness of treble side (left) is greater than that of bass side (right) because of the existence of sound-post. According to Mclennan (2008), k_1 and k_2 in Fig. 2 are set to 70 kN/m and 40 kN/m, respectively. Since the violin plate is much stiffer in horizontal direction than in vertical direction, we assume the displacement in horizontal direction is fixed for simplicity. The vibration force from strings acts along the line of bowing which is tangential to the upper curve. The side-to-side rocking motion of a bridge is proportional to tension of strings, bowing force, and bowing speed. In this study, we assume that the magnitude of bowing force remains same. Angles of bowing direction at G, A, D and G are given to 30, 11.5, −6.0 and −20.5°, respectively. Note that bowing

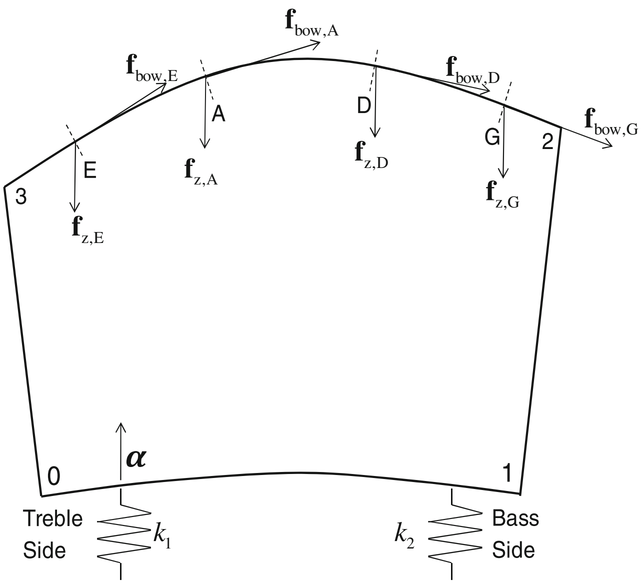

Fig. 4 Design domain and boundary condition for a violin bridge

direction along the upper edge (lines 2–3 in Fig. 4) is almost fixed in all violins since it influences the playability of a violin.

Figure 5 shows a finite element model for analysis. The bottom, black part is a non-designable domain because two foots should be exactly placed on the bass-bar and sound-post of a violin top plate. A total of 1200 (30 $\times$ 40) shell elements in ANSYS are used. The base thickness of a violin bridge tapers from 4.4 mm at the bottom to 1.4 mm at the top. Material properties of a typical maple for a bridge are shown in Table 2.

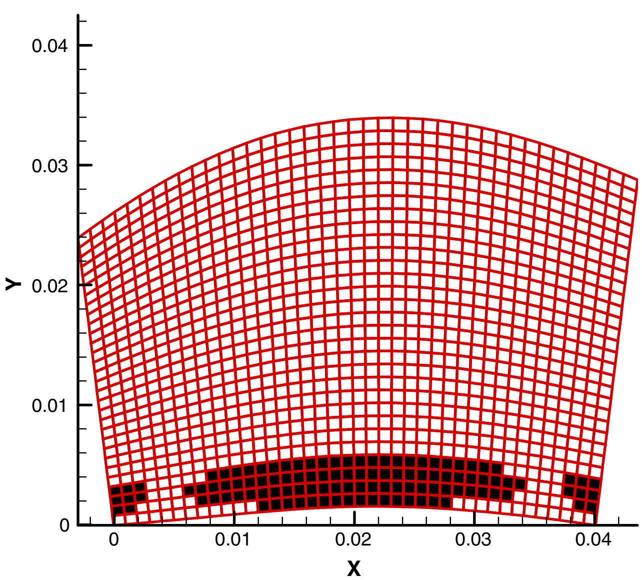

Fig. 5 Finite element model of initial violin bridges

Table 2 Material properties of maple

E_x	8.92 GPa	ν_{xy}, ν_{yz}	0.14
E_y, E_z	2.62 GPa	ν_{zx}	0.447
G_{xy}, G_{zx}	1.91 GPa	ρ_0	556 kg/m^3
G_{yz}	1.149 GPa		

3.2 Formulation and results

As widely used in SIMP method (Bendsoe 1989), the "relative" volume usage of each finite element, μ_e, is taken as a design variable. Then, elastic modulus and density of the e-th finite element, E_e and ρ_e respectively, can be expressed as

$$E_e = E_0 \mu_e^p, \quad \rho_e = \rho_0 \mu_e \tag{20}$$

where $0 < \mu_e \leq 1$, E_0 and ρ_0 are base elastic modulus and density (see Table 2), and p is a penalization factor (3 in this paper). To remove localized eigenmodes in low density areas, the modified form of SIMP method (Pedersen 2000) is used as

$$E_e = \begin{cases} E_0 \mu_e^p & \mu_c < \mu_e \leq 1 \\ \mu(\mu_c^{p-1} E_0) & \mu_{lb} < \mu_e \leq \mu_c \end{cases} \tag{21}$$

where μ_c is 0.25 in this work.

We set objective functions as maximizing the band-averaged frequency response in the range of a bridge hill (or so-called brilliant range). Several types of constraints are also considered for the design of a violin bridge. First, the structure of a violin bridge should be stiff enough to hold the strings and keep them at the right distance from the fingerboard. In the optimization formulation, the compliance is constrained to be bigger than that of a typical modern violin bridge. Second, the lowest in-plane resonance (i.e., side-to-side rocking motion of the top portion) of a violin bridge is subjected to around 3.0 kHz (i.e., the center frequency of a bridge hill) for obtaining meaningful designs. Finally, we consider a constraint of total mass of the structure because the bridge has to be light in order not to lose vibration energy during force transmission and therefore not to affect the string-body impedance.

The optimization formulation can be written as

$$\begin{aligned} \text{Maximize} \quad & S_D + S_E - S_C - S_F \\ \textit{subject to} \quad & \mathbf{f}_i^T \mathbf{u}_i \leq C_i \\ & 0.95\lambda_1 < \lambda_1 < 1.05\lambda_1 \\ & \int_\Omega \rho_0 \mu_e \mathrm{d}\Omega \leq M_0 \\ & 0 < \mu_e \leq 1 \end{aligned} \tag{22}$$

where S_i is the band-averaged response of harmonic analysis in the frequency domain i with the bridge feet resting,

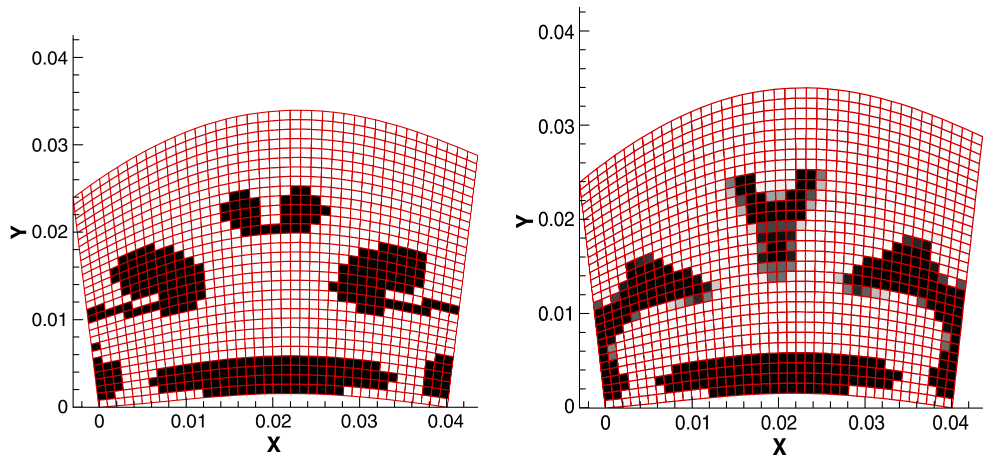

Fig. 6 Comparison of a typical bridge (left side) and optimized bridge (right side) for maximizing a bridge hill

Table 3 Various performance measures for the topology optimization of violin bridges

	Notations	Descriptions	Equations
Compliance	C_y	y directional compliance	$\mathbf{u}^T \mathbf{f}_y$
	C_z	z directional compliance	$\mathbf{u}^T \mathbf{f}_z$
	C_{bow}	Bowing direction compliance	$\mathbf{u}^T \mathbf{f}_{\mathrm{bow}}$
Dynamic properties	nf_1	The first eigenfrequency	λ_1
Band-averaged strength	S_A	Average response in base region (190–650 Hz)	$\int \lvert \boldsymbol{\alpha}^T \mathbf{u}(\omega) \rvert d\omega$
	S_B	Average response in nasal region 1 (650–1350 Hz)	
	S_C	Average response in nasal region 2 (1360–1640 Hz)	
	S_D	Average response in brilliant region 1 (1650–2580 Hz)	
	S_E	Average response in brilliant region 2 (2590–4200 Hz)	
	S_F	Average response in harsh region (4300–7000 Hz)	
Density properties	M	Mass	$\int_\Omega \rho d\Omega$

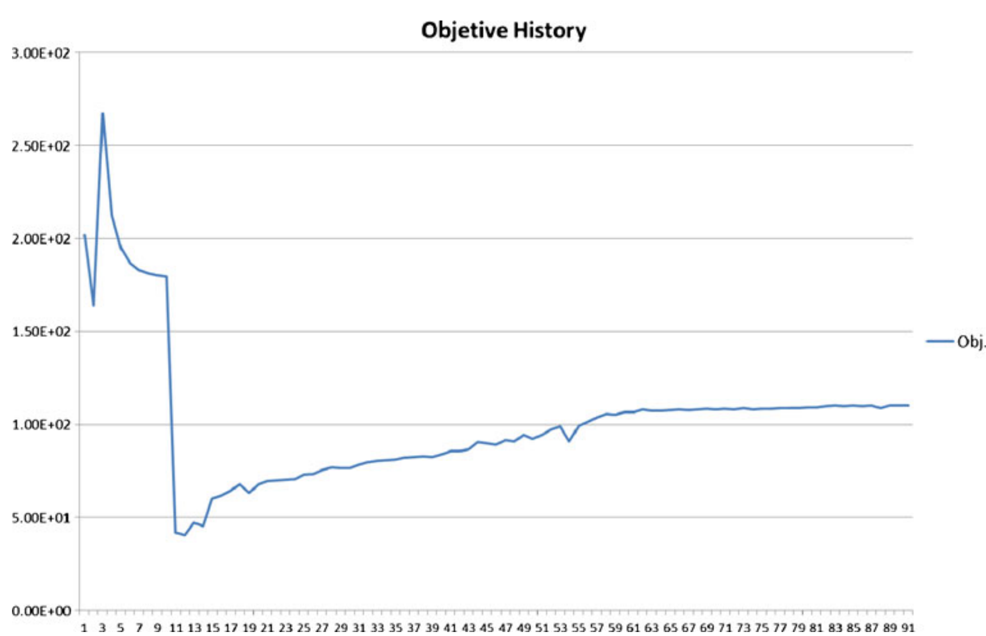

Fig. 7 Optimization history of an objective function

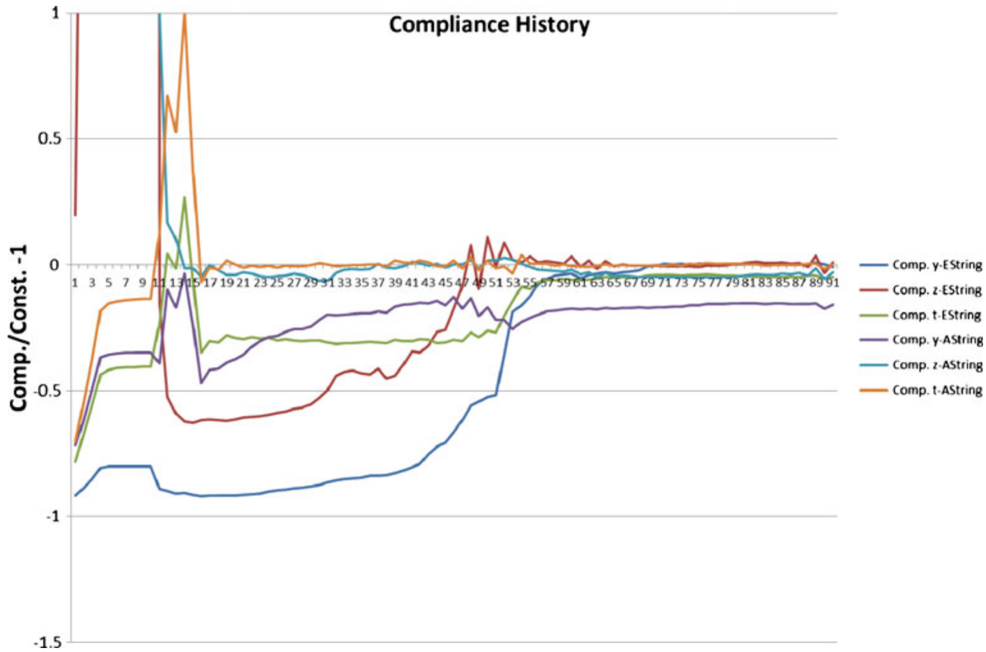

Fig. 8 Optimization history of compliance

M_0 is the maximum total mass, $\mathbf{f}_i$ and $\mathbf{u}_i$ denote the force and displacement vectors at the position i, respectively, and λ_1 the 1st eigenfrequency (3000 Hz in this paper). The limits of constraints are determined based on the corresponding performance measures of a typical violin bridge as shown in Fig. 6a. The detailed notations and formulations of performance measures are listed in Table 3.

For optimization, we chose the method of moving asymptotes (MMA) (Svanberg 1987) which has been known to be robust and very well suited for large-scale optimization with several constraints. To avoid checkerboard patterns and prevent mesh-dependency, a filtering technique (Sigmund and Petersson 1998) is also applied.

From (22) and aforementioned numerical techniques, we can obtain optimal layout of a violin bridge as shown in Fig. 6. The design for maximizing a bridge hill looks morphologically similar to a typical bridge of X shape with one hole. This result implies that the proposed design framework considering sound quality has a potential to be more realistic, so that it could be applied to tailor a bridge to one's taste. Figures 7, 8, 9 and 10 show the optimization history of an objective and constraints through iterations.

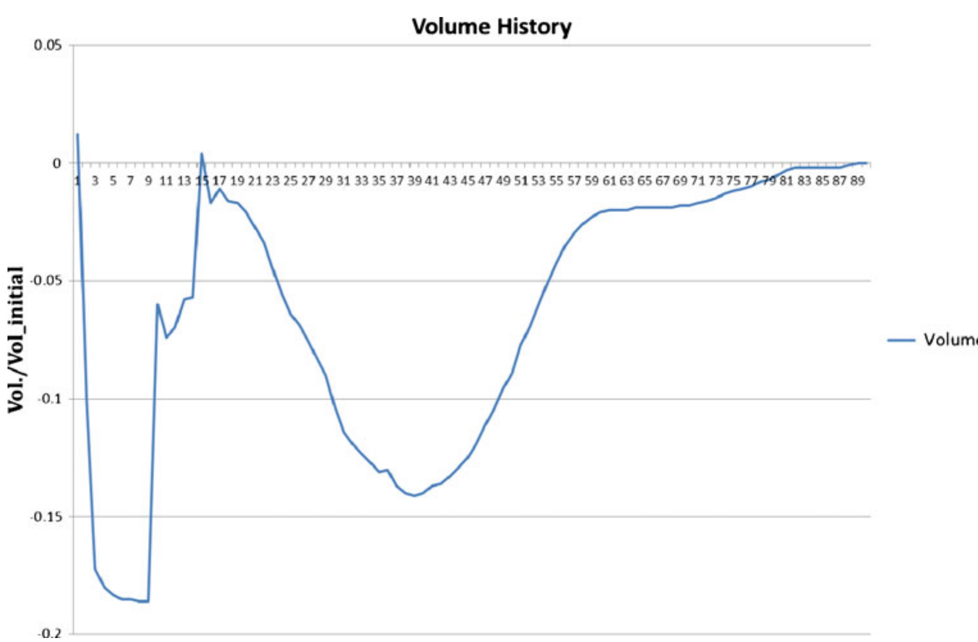

Fig. 9 Optimization history of volume

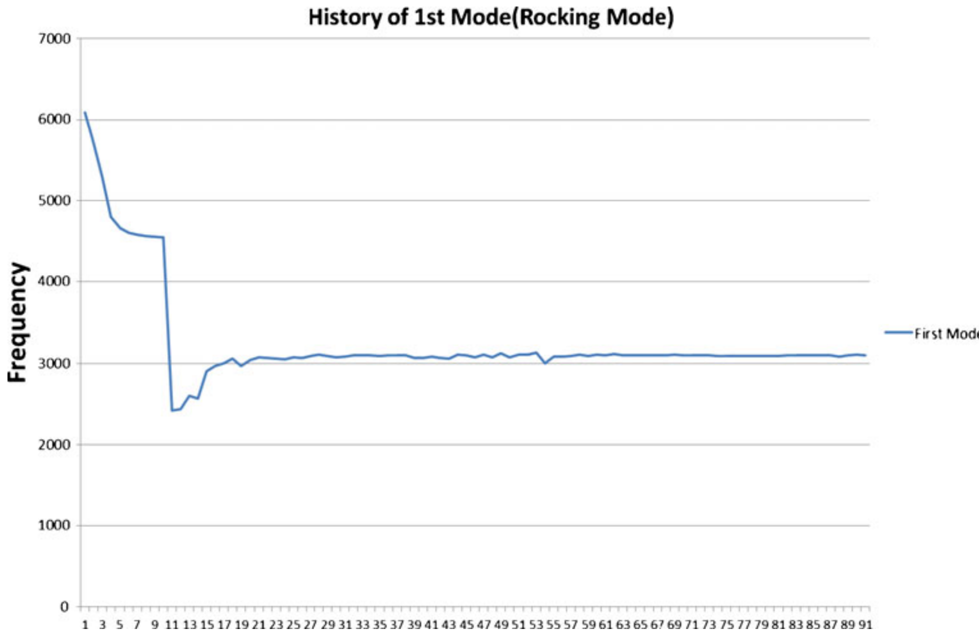

Fig. 10 Optimization history of the 1st eigenfrequency

4 Conclusion

In this study, we applied topology optimization to design a violin bridge. In order to obtain a realistic design, we proposed a band-averaged frequency response as one of acoustical parameters for sound quality based on previous related researches. The sensitivities of the proposed measure are efficiently calculated by spline approximation and regressed system matrices. The proposed method enables us to obtain the optimized violin bridge which is similar to a typical violin bridge. Numerical results show the applicability of optimization to violin design. Depending on the formulation with selected measures, we may have various designs which can satisfy the desired characteristics.

Although the vertical stiffness of a violin body in this study is fixed and obtained from the literature, the stiffness varies depending on violin makers, material, environmental condition, etc. In our future applications, the stiffness of a "given" violin body would be experimentally obtained and then be applied to optimization for more effective customization or tuning. This work would provide insight into the development of systematical design framework for tuning which has been fully based on violin maker's experiences and intuition.

Acknowledgements This research is partially supported by the Samsung Chair Endowment fund. This research is also partially supported by Basic Science Research Program through the National Research Foundation of Korea (NRF) funded by the Ministry of Education, Science and Technology (2011–0013307). We are sincerely grateful to Mr. Young Sik Jun, a violin maker at Machold Korea, for deeply advising on our works. We would also like to thank Dr. Krister Svanberg at KTH (Stockholm, Sweden) for providing the MMA code for academic research.

References

Bendsoe MP (1989) Optimal shape design as a material distribution problem. Struct Multidisc Optim 1(4):193–202

Bendsoe MP, Sigmund O (2003) Topology optimization; theory, methods, and applications. Springer

Borrvall T, Petersson J (2001) Large-scale topology optimization in 3D using parallel computing. Comput Methods Appl Mech Eng 190:6201–6229

Buen A (2003) Differences of sound spectra in violins by Stradivari and Guarneri Del Gesu. Catgut Acoust Soc J 4(8):14–18

Buen A (2007) On timbre parameter and sound levels of recorded old violins. J Violin Soc Am XXI(1):57–68

Choi KK, Kim NH (2005) Structural sensitivity analysis and optimization: linear systems. Springer

Cremer L (1983) Physics of the violin. MIT Press

Dunnwald H (1991) Deduction of objective quality parameters on old and new violins. Catgut Acoust Soc J 1:1–5

Gabrielsson A, Jansson E (1977) An analysis of long-time-average spectra of twenty-two quality rated violins. Catgut Acoust Soc Newsl 27:13–19

Geissler P, Martner O, Zerbs C, Schleske M (2003) Psychoacoustic investigations on the possiblity of aurally identical violins. In: Proc stockh music acoust conf (SMAC03), Stockholm, Sweden

Gough C (2000) Science and the stradivarius. Phys World 13(4): 27–33

Hutchins CM, Benade V (1997) Research papers in violins acoustics: 1975–1993. Acoust Soc Am, New York Woodbury

Jang IG, Kwak BM (2006) Evolutionary topology optimization using design space adjustment based on fixed grid. Int J Numer Methods Eng 66(11):1817–1840

Jang IG, Kwak BM (2008) Design space optimization using design space adjustment and refinement. Struct Multidisc Optim 35(1):41–54

Jansson EV, Niewczyk BK (1999) On the acoustics of the violin: bridge or body hill. Catgut Acoust Soc J 4:23–27

Jensen JS (2007) Topology optimization of dynamics problems with padé approximants. Int J Numer Methods Eng 72(13):1605–1630

Kim TS, Kim YY (2000) Mac-based mode-tracking in structural topology optimization. Comput Struct 74(3):375–383

Ma ZD, Kikuchi N, Hagiwara I (1993) Structural topology and shape optimization for a frequency response problem. Comput Mech 13(3):157–174

Ma ZD, Kikuchi N, Cheng HC, Hagiwara I (1995a) Topological optimization technique for free vibration problem. J Appl Mech 62(1):200–207

Ma ZD, Kikuchi N, Cheng HC (1995b) Topological design for vibrating structures. Comput Methods Appl Mech Eng 121(1–4): 259–280

Mclennan JE (2008) The violin music acoustics from baroque to romantic. Doctorial thesis, School of Physics, University of New South Wales

Moral JA, Jansson EV (1978) Long-time-averaged-spectra of scales and spectra of single tones from a violin. STL-QPSR 1/1978

Müller HA (1979) The function of the violin bridge. Catgut Acoust Soc Newsl 31:19–22

Pedersen NL (2000) Maximization of eigenvalues using topology optimization. Struct Multidisc Optim 20(1):2–11

Schleske M (2010) On making 'Tonal Copies' of a violin. http://www.schleske.de/fileadmin/user_upload/doc/CAS_Tonal_Copies.pdf. Accessed 10 Mar 2010

Sigmund O, Petersson J (1998) Numerical instabilities in topology optimization: a survey on procedures dealing with checkerboards, mesh-dependencies and local minima. Struct Multidisc Optim 16(1):68–75

Silva E, Nishiwaki S, Kikuchi N (2000) Topology optimization design of flextensional actuators. IEEE Trans Ultrason Ferroelectr Freq Control 47(3):657–671

Stepanek J, Otcenasek Z (1999) Rustle as an attribute of timbre of stationary violin tones. Catgut Acoust Soc J 3(8):32–38

Stepanek J, Otcenasek Z (2001) Psychoacoustic aspects of violin sound quality and its spectral relations. In: 17th int congr acoust, Rome, Italy

Stepanek J, Otcenasek Z (2004) Interpretation of violin spectrum using psychoacoustic experiments. In: Int symp music acoust, Japan

Stepanek J, Otcenasek Z (2005) Acoustical correlates of the main features of violin timbre perception spectrum using psychoacoustics experiments. In: Proc conf interdicip music, Montreal, Canada

Stolpe M, Svanberg K (2001) An alternative interpolation scheme for minimum compliance topology optimization. Struct Multidisc Optim 22(2):116–124

Svanberg K (1987) The method of moving asymptotes—a new method for structural optimization. Int J Numer Methods Eng 24(2): 359–373

Woodhouse J (2005) On the "bridge hill" of the violin. Acta Acust United Acuast 91(1):155–165

Yang RJ, Chuang CH (1994) Optimal topology design using linear programming. Comput Struct 52:265–275

Yoo J, Kikuchi N (2002) Topology optimization for reduction of vibration caused by magnetic harmonic excitation. IEEE Trans Magn 38(6):3643–3649

Yoon GH (2010) Structural topology optimization for frequency response problem using model reduction schemes. Comput Methods Appl Mech Eng 199:1744–1763

Yu YG, Kwak BM (2011) Design sensitivity analysis of acoustical damping and its application to design of musical bells. Struct Multidisc Optim 44:421–430

Yu YG, Jang IG, Kim IK, Kwak BM (2010) Nodal line optimization and its application to violin top plate design. J Sound Vib 329(22):4785–4796